HHS Public Access

Author manuscript

Neuron. Author manuscript; available in PMC 2019 May 02.

Published in final edited form as:

Neuron. 2018 May 02; 98(3): 562–574.e5. doi:10.1016/j.neuron.2018.03.039.

Activation of $G_{\alpha q}$ signaling enhances memory consolidation and slows cognitive decline

Rachel N. Arey[1,2], **Geneva M. Stein**[1,2], **Rachel Kaletsky**[1,2], **Amanda Kauffman**[1,2], and **Coleen T. Murphy**[1,2,3,*]

[1]Lewis- Sigler Institute for Integrative Genomics, Princeton University, Princeton, NJ 08544, USA

[2]Department of Molecular Biology, Princeton University, Princeton, NJ 08544, USA

Summary

Perhaps the most devastating decline with age is the loss of memory. Therefore, identifying mechanisms to restore memory function with age is critical. Using *C. elegans* associative learning and memory assays, we identified a gain-of-function $G_{\alpha q}$ signaling pathway mutant that forms a long-term (CREB-dependent) memory following one Conditioned Stimulus-Unconditioned Stimulus (CS-US) pairing, which usually requires seven CS-US pairings. Increased CREB activity in AIM interneurons reduces the threshold for memory consolidation through transcription of a set of previously-identified "long-term memory" genes. Enhanced $G_{\alpha q}$ signaling in the AWC sensory neuron is both necessary and sufficient for improved memory and increased AIM CREB activity, and activation of $G_{\alpha q}$ specifically in aged animals rescues the ability to form memory. Activation of $G_{\alpha q}$ in AWC sensory neurons cell-non-autonomously induces consolidation after one CS-US pairing, enabling both cognitive function maintenance with age and restoration of memory function in animals with impaired memory performance, without decreased longevity.

eTOC Blurb

Arey et al., have found that activating the $G_{\alpha q}$ signaling pathway in sensory neurons enhances memory in young animals utilizing the canonical CREB pathway. This pathway also slows age-related memory loss and reverses age-related memory impairment.

Introduction

Although life expectancy is increasing (Lenart and Vaupel, 2017), therapies to treat age-related memory decline are lacking, creating a growing public health threat. Cognitive

*Correspondence to: ctmurphy@princeton.edu.
[3]Lead Contact

Author Contributions: R.A and C.T.M designed experiments. R.A., G.S., R.K., and A.K. performed experiments and analyzed data. R.A., G.S. and A.K. performed behavioral experiments. R.A. and R.K. performed microarray analysis. R.A., R.K., and A.K. performed microscopy experiments. R.A. performed qPCR experiments. R.A. and C.T.M. wrote the manuscript.

Declaration of Interests: The authors declare no competing interests.

function decreases in mid-life and worsens with age (Park et al., 2002). These deficits are caused by subtle changes in the plasticity of circuits that regulate learning and memory (Arey and Murphy, 2017; Burke and Barnes, 2006), which may provide insight into critical mechanisms involved in memory formation and targets for the prevention of age-related cognitive decline. Recent studies have identified interventions that have memory-promoting effects in aged rodents. For example, young blood parabiosis improves hippocampal-dependent learning and memory in aged mice (Villeda et al., 2014). Aged mice receiving chronic, systemic administration of low-dose tetrahydrocannabinol (THC) also display better spatial learning and long-term memory than vehicle-treated controls (Bilkei-Gorzo et al., 2017). Improved memory performance with both of these treatments is accompanied by molecular and cellular changes, including increased spine density, elevated expression of plasticity-related genes, and increased CREB transcriptional activity (Bilkei-Gorzo et al., 2017; Villeda et al., 2014). Interestingly, these treatments selectively improve memory in aged mammals, and either have no effect (Villeda et al., 2014) or can impair memory (Bilkei-Gorzo et al., 2017) in young animals. Ideally, potential therapeutics would have benefits in both younger and aged individuals, since cognitive performance in humans begins to decline relatively early in their lifespan (Park et al., 2002).

Like mammals, *C. elegans* can form associative memories, requiring conserved molecular machinery to learn and remember (Kauffman et al., 2010; Lakhina et al., 2015; Shen et al., 2014; Stein and Murphy, 2014; Vukojevic et al., 2012). Furthermore, associative learning and memory deficits are the earliest features of neuronal aging in *C. elegans*, preceding age-related changes in neuronal morphology, motility, chemotaxis, and other behaviors (Arey and Murphy, 2017; Kauffman et al., 2010). The processes that regulate memory performance with age in *C. elegans* appear to also be highly conserved. CREB levels and activity correlate with long-term associative memory (LTAM) performance with age (Kauffman et al., 2010), similar to what has been observed in mammals (Kudo et al., 2005). Maintenance of presynaptic vesicle transport and release is also important for learning and memory in both young and aged animals (Kaletsky et al., 2016; Li et al., 2016). Components of this pathway are necessary for the extended short-term associative memory (STAM) of long-lived *C. elegans daf-2* insulin receptor mutants, and important for their enhanced learning with age (Kaletsky et al., 2016; Kauffman et al., 2010; Li et al., 2016), and increased synaptic density and plasticity coincide with the beneficial effects of THC and young-blood parabiosis (Bilkei-Gorzo et al., 2017; Villeda et al., 2014). Thus, conserved molecules that enhance synaptic function and regulate CREB activity may present new targets for the treatment of cognitive decline.

The $G_{\alpha q}$ signaling pathway is one of the main positive regulators of presynaptic transmission in *C. elegans*. The *C. elegans* $G_{\alpha q}$ homolog EGL-30 (Brundage et al., 1996) promotes both neurotransmission (Lackner et al., 1999; Miller et al., 1999) and neuropeptide secretion (Ch'ng et al., 2008) via DAG-Rho signaling (Figure 1A). $G_{\alpha q}$ signaling has been implicated in a number of *C. elegans* processes, including locomotion, egg-laying, adaptation, and learned salt avoidance (Adachi et al., 2010; Brundage et al., 1996; Matsuki et al., 2006), as well as working memory in mammals (Frederick et al., 2012), but the role of $G_{\alpha q}$ in long-term memory in *C. elegans* and higher organisms is untested.

Here we report that activation of $G_{\alpha q}$ signaling, which increases presynaptic transmission, lowers the threshold for memory consolidation in young animals so that a long-term memory, which usually requires 7 CS-US pairings, is formed after only a single CS-US pairing. A single sensory neuron pair, the AWC, is the site of $G_{\alpha q}$ signaling that is both necessary and sufficient for enhanced consolidation, and AWC-specific activation of $G_{\alpha q}$ signaling slows age-related decline in memory performance. Furthermore, increasing activity of the $G_{\alpha q}$ signaling pathway in the AWC of aged animals that already exhibit cognitive impairment restores the ability to form long-term memories. This improved memory performance is due to cell non-autonomous $G_{\alpha q}$ signaling regulation of CREB activity in the AIM via neuropeptide signaling, which increases the transcription of a previously identified set of CREB/LTAM training-dependent genes (Lakhina et al., 2015). Moreover, activation of $G_{\alpha q}$ signaling specifically in the AWC enhances memory without the lifespan decrease caused by $G_{\alpha q}$ activation in the whole body. Activation of this conserved $G_{\alpha q}$ signaling pathway is a new mechanism to improve memory performance in young and aged animals, and may present a target for the development of future therapies that treat age-related cognitive decline.

Results

EGL-30 gain-of-function mutants exhibit enhanced memory consolidation

We hypothesized that the $G_{\alpha q}$ signaling pathway (Figure 1A), which regulates synaptic transmission and olfactory adaptation, another associative behavioral paradigm (Matsuki et al., 2006), might play a role in associative learning and memory. We subjected $G_{\alpha q}$ signaling component mutants to positive olfactory associative training for both short-term (1 CS-US pairing) and long-term memory (7CS-US pairings) (Kauffman et al., 2010). Hypomorphic *egl-30*/$G_{\alpha q}$ mutants display a mild defect in learning (Figure S1A) after 1 CS-US pairing and are unable to form short-term memory (Figure 1A, S1B). Genetic ablation of other components of $G_{\alpha q}$ signaling, including *egl-8*/PLCβ (Figure 1A, S1D), *unc-73*/Trio GEF (Figure 1A, S1F), and *pkc-1*/PKCε (Figure 1A, S1H), and $G_{i/o}$/*goa-1*(Figure 1A, S1J) resulted in defective learning after 1 CS-US pairing. $G_{\alpha q}$ signaling is also necessary for forming associations after long-term memory training, as all mutants tested in the pathway showed defective learning after 7 CS-US pairings (Figure 1A, S1C,E,G,I), obscuring any effects the proteins may have on long-term memory (Lakhina et al., 2015).

Because $G_{\alpha q}$ signaling is essential for normal associative learning and memory, we reasoned that increasing the activity of this pathway may enhance memory performance and improve memory function with age. To test this hypothesis, we subjected animals with a gain-of-function (*js126*) mutation in *egl-30* to positive olfactory associative memory training (Kauffman et al., 2010). *egl-30(js126)* mutants have a single G-to-A transition that results in Methionine rather than Valine incorporation at amino acid 180 (V180M) in the GTPase domain (Hawasli et al., 2004), altering EGL-30's endogenous GTPase activity (Hawasli et al., 2004). Remarkably, *egl-30(js126)* mutants exposed to a single pairing of the neutral odorant butanone (CS) with food (US), which normally results in short-term memory that decays over the course of two hours (Figure 1B, S1K; (Kauffman et al., 2010), exhibited a

>10-fold memory extension, lasting more than 24 hours, following a single CS-US pairing (Figure 1B, S1K).

EGL-30 gain-of-function mutants increase memory duration via increased CREB activity

egl-30(js126)'s dramatic extension of memory duration resembled LTAM, which usually requires spaced training of at least 7 CS-US pairings (Kauffman et al., 2010) and the activity of the transcription factor CREB/*crh-1.* CREB is a conserved regulator of LTAM in a number of organisms, including *C. elegans* (Kauffman et al., 2010; Lakhina et al., 2015; Silva et al., 1998), but is not required for short- or intermediate-term memory [S/ITAM] (Kauffman et al., 2010). *egl-30(js126)*'s extended one CS-US pairing memory indeed required CREB: *egl-30(js126);crh-1(tz2)* double mutants no longer maintained an extended positive butanone association (Figure 1C), indicating that CREB-dependent LTAM is formed after one CS-US pairing.

How might consolidation, which usually requires multiple rounds of spaced training, occur after a single CS-US pairing when $G_{\alpha q}$ activity is elevated? Consolidation can be enhanced by increasing CREB levels or by indirectly stimulating CREB activity in *C. elegans, Drosophila,* and mammals (Josselyn et al., 2001; Kauffman et al., 2010; Sekeres et al., 2012; Yin et al., 1995). Using a *pCRE::GFP* transgenic reporter of CREB activity (Suo et al., 2006), we found that naïve (untrained) *egl-30(js126);pCRE::GFP* animals exhibited GFP fluorescence in the AIM and SIA interneurons (Figure 1D–E), a pattern resembling wild-type *pCRE::GFP* worms after 7 CS-US pairings (7× trained, Figure 1D; (Lakhina et al., 2015)). Therefore, *egl-30(js126)* animals display CREB activation under conditions (1 CS-US pairing) that would not normally activate CREB.

EGL-30 gain-of-function mutants maintain the ability to form long-term memories with age

By day 4–5 of adulthood, wild-type *C. elegans* lose their LTAM ability, and learning and S/ITAM decline quickly thereafter (Kauffman et al., 2010). CREB levels and activity correlate with LTAM ability with age (Kauffman et al., 2010). We examined whether high CREB activity in *egl-30(js126)* mutants conferred LTAM ability with age: at Day 5 of adulthood, *egl-30(js126)* mutants still exhibited LTAM after one CS-US pairing (Figure 1F), whereas wild-type animals exhibit no LTAM after 7CS-US pairings (Kauffman et al., 2010). To confirm that this was indeed LTAM formation, rather than the development of a butanone preference with age, Day 5 wild-type animals were tested after one CS-US pairing; they exhibited no detectable change in butanone preference at the LTAM timepoint (16 hours post training, Figure 1F), indicating that *egl-30(js216)* animals indeed maintain the ability to form associative memories.

We found that LTAM ability correlated with maintenance of CREB activity in the AIM interneurons of aged (Day 5) *egl-30(js126);pCRE::GFP* animals (Figure 1G, H). Though CREB activity is elevated in both young and aged *egl-30(js126)* mutants, their *crh-1* mRNA levels are similar to wild-type animals (Figure S2A–B), suggesting that EGL-30 activity increases CREB's activity rather than its transcription.

AIM CREB activity is required for enhanced consolidation in *egl-30(js216)* mutants

We next determined where CREB activity is required for *egl-30(js126)'s* enhanced memory. AIM interneurons, and CREB activation in AIM interneurons (but not SIA neurons), is required for long-term memory formation after 7 CS-US pairings (Lakhina et al., 2015). We found that although CREB activity is elevated in the SIA after training (Figure 1D), SIA-specific CREB rescue in *egl-30(js126);crh-1(tz2)* animals failed to restore memory (Figure 2A), while rescue of CREB activity in the AIM restored LTAM ability to *egl-30(js216);crh-1(tz2)* mutants (Figure 2B). The requirement for CREB in the AIM interneurons is in agreement with the previous observation that rescue of *crh-1*/CREB in the AIM interneurons, but not the SIA neurons, rescues the ability to form long-term memories in *crh-1(tz2)* mutants (Lakhina et al., 2015).

Increased AIM CREB activity leads to elevated transcription of CREB/LTAM-dependent genes in naïve animals

Following LTAM training in wild-type animals, increased CREB activity in the AIM induces the expression of a set of 757 CREB-dependent/LTAM training-dependent genes (Lakhina et al., 2015). The increased expression of these genes is specific to CS-US pairings, because mock training (where animals undergo 7 rounds of training in the absence of the odorant (CS)) has no detectable effect on these CREB/LTAM genes (Lakhina et al., 2015). Their expression is also unaffected by unpaired odorant exposure (Lakhina et al., 2015). The induction of this CREB/LTAM gene set is not merely indicative of memory training, but is also required for normal memory formation; reducing the activity of many of these genes, either through loss-of function mutation or RNAi treatment, causes long-term memory impairment (Lakhina et al., 2015).

Because CREB activity in the nervous system of naïve *egl-30(js126)* animals resembled that of wild-type animals following LTAM training, we asked whether elevated CREB activity in the AIM interneurons induces the expression of CREB/LTAM-dependent genes (Lakhina et al., 2015) in *egl-30(js126)* animals, prior to conditioning. Microarray analysis of untrained *egl-30(js126)* worms and wild-type worms revealed that in the naïve state, *egl-30(js126)* animals have a CREB/LTAM-dependent gene expression pattern strikingly similar to LTAM-trained wild-type animals (Pearson correlation = 0.56; Figure 2C), suggesting that elevated CREB activity and downstream target gene expression prior to training could permit LTAM formation after a single training session. Training did not further increase GFP fluorescence in *egl-30(js126);pCRE::GFP* animals for up to 6 hours after conditioning (Figures 1D, 2D, and S2C), suggesting that CREB activity is not further elevated following training. Therefore, naïve CREB activation and subsequent upregulation of CREB/LTAM genes may be sufficient for long-term memory formation in *egl-30(js126)* animals.

Elevated CREB-mediated transcription in naïve EGL-30 gain-of-function mutants is sufficient for long-term memory formation

LTAM requires new transcription and is blocked by actinomycin D treatment (Kauffman et al., 2010; Vukojevic et al., 2012). To test whether the pre-existing elevated transcription of CREB/LTAM-dependent genes observed in *egl-30(js126)* animals was sufficient to induce LTAM, we treated *egl-30(js126)* worms with actinomycin D during the training paradigm.

Blocking new transcription (Figure S2D) does not affect learning or LTAM in *egl-30(js126)* worms (Figures 2E, S2E), indicating that they are already "primed" for LTAM without the need for new transcription. By contrast, cycloheximide treatment during training of *egl-30(js126)* prevents LTAM, suggesting that translation of the naïve transcriptional state is necessary for memory consolidation in *egl-30(js126)* (Figures 2F, S2F).

Increased $G_{\alpha q}$ signaling in the AWC sensory neuron is necessary and sufficient for enhanced memory consolidation

egl-30(js126) mutants express constitutively active EGL-30 throughout the animal; therefore, we next sought to identify the site of EGL-30 activity that results in CREB activation and enhanced consolidation. *egl-30(js126)'s* LTAM only required training (1 CS-US) that usually forms S/ITAM, so we hypothesized that EGL-30 acts in neurons required for both LTAM and S/ITAM forms of memory. CREB activity is necessary in the AIM interneurons for LTAM (Lakhina et al., 2015), but is not necessary for S/ITAM ((Lakhina et al., 2015); Figure S3D). Butanone is sensed by the AWC sensory neuron (Bargmann et al., 1993), which is required for both LTAM and S/ITAM. The AIA interneuron is the sole interneuron directly connected to the AWC that synapses onto the AIM (Chen et al., 2006); although the AIA/AIY is required upstream of CREB activity in the AIM for LTAM formation in wild-type animals (Figures S3A–C), like AIM, it is not required for S/ITAM (Figure S3E). We therefore examined whether activation of $G_{\alpha q}$ signaling solely in the AWC would affect memory consolidation.

We tested two constitutively active forms of EGL-30 (Q205L and V180M) under an AWC-specific promoter (*Podr-1)*, and found that activation of $G_{\alpha q}$ in this neuron was sufficient to extend memory following one CS-US pairing to a degree that was indistinguishable in duration from *egl-30(js126)* animals (Figures 3A, S3F–G). To verify that the extended memory we observed in animals expressing an AWC-specific gain-of-function EGL-30 was due to elevated $G_{\alpha q}$ signaling, we examined the memory ability of *egl-8(n488);Podr-1::egl-30(Q205L)* mutants, which lack PLCβ activity downstream of EGL-30. *egl-8(n488)* suppresses *Podr-1::egl-30(Q205L)'s* extended memory (Figure 3B), indicating that the memory phenotype of *Podr-1::egl-30(Q205L)* was due to increased $G_{\alpha q}$ signaling in the AWC sensory neuron.

Although increased $G_{\alpha q}$ signaling in the AWC sensory neuron should increase synaptic transmission, it does not alter butanone sensation in the animal: *Podr-1::egl-30(Q205L), egl-30(js126),* and wild-type animals display normal naïve butanone chemotaxis (Figures S4A–B), indicating that increased butanone preference only occurs in the context of behavioral conditioning. Furthermore, training increases *egl-30(js126)'s* preference for butanone, but not benzaldehyde, another AWC-sensed odorant, at the memory timepoint, indicating that memory is specific to the CS (butanone) and not due to a general increase in AWC activity (Figure S4C).

Podr-1::egl-30(Q205L) worms' memory was also CREB-dependent (Figure 3C), and required LTAM-specific neurons, the AIM and AIA/AIY (Figure 3D–E). Therefore, AWC-specific activation of $G_{\alpha q}$ signaling is sufficient to induce LTAM following a single CS-US pairing. Moreover, repressing $G_{\alpha q}$ signaling in the AWC of *egl-30(js126)* animals via

targeted expression of a constitutively active negative regulator of $G_{\alpha q}$, *goa-1*, abolished LTAM (Figure 3F), despite the fact that $G_{\alpha q}$ signaling was enhanced elsewhere in the nervous system. Furthermore, learning and STAM remained intact (Figure S4D–E) in *egl-30(js126);Podr-1::goa-1(Q205L)* animals, indicating that the effects of inhibiting the enhanced $G_{\alpha q}$ signaling were specific to LTAM. $G_{\alpha q}$ signaling in the AWC is not only necessary, but sufficient for enhanced consolidation.

Increased $G_{\alpha q}$ signaling in the AWC sensory neuron results in cell non-autonomous regulation of CREB activity in the AIM

The enhanced memory consolidation observed in *egl-30(js126)* animals is due to elevated CREB activity specifically in the AIM interneurons (Figure 1D–E, 2B). Because increased $G_{\alpha q}$ signaling specifically in the AWC also resulted in the formation of a long-term memory after one CS-US pairing, we hypothesized that AIM CREB activity may be regulated cell non-autonomously by $G_{\alpha q}$ signaling in the AWC. To test this, we examined *pCRE::GFP* reporter activity in animals with an AWC-specific, gain-of-function EGL-30 (*Podr-1::egl-30(V180M);pCRE::GFP),* and found that increased $G_{\alpha q}$ signaling solely in the AWC was sufficient to increase CREB activity in the AIM in naïve (untrained) animals, similar to that observed in *egl-30(js126)* mutants (Figure 4A–B).

Increased neuropeptide secretion from the AWC is necessary and sufficient for enhanced memory

We next investigated how $G_{\alpha q}$ signaling in the AWC might cell non-autonomously regulate CREB activity. $G_{\alpha q}$ signaling positively regulates both neurotransmission and neuropeptide secretion (Ch'ng et al., 2008; Lackner et al., 1999; Miller et al., 1999). To determine which signal from the AWC is necessary for enhanced consolidation, we expressed RNAi targeting either the vesicular glutamate transporter *eat-4,* which is required for neurotransmission, or *unc-31*, which is required for neuropeptide secretion (Leinwand and Chalasani, 2013; Sieburth et al., 2007), in the AWC of *egl-30(js126)* mutants. Reduction of glutamatergic (neurotransmission) signaling from the AWC did not affect *egl-30(js126)* memory (Figure S4F), but neuropeptide signaling was required, as *unc-31* reduction impairs LTAM (Figure 4C). We next examined if the requirement for neuropeptidergic signaling from the AWC was specific to enhanced memory, or was also necessary for normal long-term memory. We found that AWC-specific knockdown of *unc-31* in wild-type animals resulted in a long-term memory deficit without any effect on learning (Figure 4D, S4G). This result further supports the hypothesis that elevated $G_{\alpha q}$ signaling enhances memory consolidation through increased activity of pathways necessary for normal long-term memory formation.

We next examined if increasing neuropeptide release from the AWC was sufficient to enhance memory. To test this hypothesis, we expressed a gain-of-function PKC-1(A160E), which selectively regulates the release of neuropeptide-containing dense-core vesicles, specifically in the AWC of wild-type animals (Dekker et al., 1993; Sieburth et al., 2007; Tsunozaki et al., 2008). We found that animals expressing this AWC-specific, gain-of-function PKC-1 exhibited an extended (24hr) memory after one CS-US (Figure 4E) pairing, indicating that increased neuropeptide secretion from the AWC is sufficient for enhanced memory.

Increasing $G_{\alpha q}$ signaling in the AWC of aged animals rescues impaired memory function

We next determined whether enhanced $G_{\alpha q}$ signaling in the AWC alone was sufficient for memory maintenance with age. Animals expressing two different constitutively active forms (Q205L or V180M) of EGL-30 in the AWC exhibited LTAM following one CS-US pairing at Day 5 of adulthood (Figures 5A, S5A). This memory maintenance also correlated with maintenance of elevated CREB activity in the AIM interneurons of aged (Day 5) *Podr-1::egl-30(V180M); pCRE::GFP* animals (Figure 5B–C). While whole-life activation of $G_{\alpha q}$ signaling in the AWC slows age-related cognitive decline, we wondered if there were any beneficial effects of increasing $G_{\alpha q}$ signaling in the AWC specifically in aged animals, as wild-type worms can no longer form LTAM by Day 4 (Kauffman et al., 2010). We utilized a FLP recombinase driven by a heat-shock protein (*hsp-16.48)* promoter (Davis et al., 2008) to permanently activate a FLP-inducible form of a GFP-tagged, constitutively active EGL-30 in the AWC (*HS Inducible Podr-1::egl-30(Q205L))*. This inducible EGL-30 (Figure 5D) was functional: early larval L1 animals subjected to heat shock exhibited LTAM after one CS-US pairing at Day 1 of adulthood, similar to worms expressing EGL-30(Q205L) in the AWC throughout their whole lifetime (Figures 5E, S5B). To examine the effects of activation of $G_{\alpha q}$ signaling in the AWC specifically in aged animals, we induced EGL-30(Q205L) expression in *HS Inducible Podr-1::egl-30(Q205L)* animals on Day 4 of adulthood, and compared their behavior following one CS-US pairing at Day 5 of adulthood to both wild-type siblings or *HS Inducible Podr-1::egl-30(Q205L)* animals without transgene induction (see Figure 5F for schematic). While both wild-type siblings and *HS Inducible Podr-1::egl-30(Q205L)* animals without transgene induction were unable to form memory (Figures 5G, S5C), the induction of AWC-specific activation of $G_{\alpha q}$ signaling at Day 4 of adulthood rescued the ability to form LTAM (Figures 5H, S5D). Thus, increased $G_{\alpha q}$ signaling in the AWC rescues LTAM in aged animals with impaired memory.

AWC-specific $G_{\alpha q}$ signaling improves memory without decreasing lifespan

Although increased $G_{\alpha q}$ signaling allows maintenance of cognitive performance with age, it has also been associated with a decrease in lifespan, as *egl-30(js126)* mutants exhibit decreased lifespan (Ch'ng et al., 2008). Because increased $G_{\alpha q}$ signaling in the AWC is sufficient to improve memory and slow cognitive decline, we examined its effects on longevity. As previously reported (Ch'ng et al., 2008), *egl-30(js126)* mutants are short-lived (Figure 5I); however, animals expressing either Q205L or V180M gain-of-function alleles of *egl-30* specifically in the AWC have a normal lifespan (Figure 5I, S5E). Therefore, identification of the neural site of $G_{\alpha q}$ signaling-mediated memory consolidation enables memory improvement without compromising longevity.

Discussion

Here we identified $G_{\alpha q}$ signaling as a novel positive regulator of memory consolidation. This function is unlikely to be limited to *C. elegans*, as EGL-30 shares 82% identity with the mammalian GNAQ (Brundage et al., 1996). While $G_{\alpha q}$ signaling has been implicated in *C. elegans* associative behaviors (Matsuki et al., 2006) and in mammalian working memory (Frederick et al., 2012), it has not been specifically identified as a long-term memory regulator in higher organisms. We provide the first direct evidence that $G_{\alpha q}$ regulates

associative memory. The downstream targets of $G_{\alpha q}$ have also been implicated in cognitive function in higher organisms. Loss of PLCβ/EGL-8 and TRIO/UNC-73 have been linked to deficits in working memory and learning in mice, respectively (Kim et al., 2015; Zong et al., 2015). PKC isoforms play an essential role in mammalian learning and memory (Abeliovich et al., 1993; Sacktor and Hell, 2017; Sun and Alkon, 2014; Sutton et al., 2004; Weeber et al., 2000); however, the mammalian ortholog of *pkc-1,* PKC1ε, has not been as well characterized in memory formation. Furthermore, little is known about $G_{\alpha q}$ and its downstream targets in the context of normal aging and cognitive decline.

We found that enhanced $G_{\alpha q}$ signaling enables memory formation in aged animals, when LTAM normally no longer functions. The memory-enhancing effect of $G_{\alpha q}$ signaling in both young and old animals is due to elevated CREB activity in the AIM interneurons, and the subsequent up-regulation of a previously-identified memory gene set (Lakhina et al., 2015). The up-regulation of these CREB-dependent/training-dependent genes “primes” the animals for memory formation even in the presence of transcriptional blockage.

The correlation between memory function with age and CREB activity appears to be a highly conserved mechanism. Recently, viral-mediated overexpression of CREB in the CA1 was found to improve memory in aged, but not young, rats (Yu et al., 2017). Increased CREB activity is also involved in the memory-promoting effects of caloric restriction (Fusco et al., 2012), young blood parabiosis (Villeda et al 2014), and low-dose Δ^9-tetrahydocannabinol treatment of aged mice (Bilkei-Gorzo et al., 2017). However, here we have identified a pathway that enhances memory performance in young animals, slows cognitive decline, and rescues age-related memory impairment.

$G_{\alpha q}$ signaling influences CREB and the LTAM network cell non-autonomously (Figure 6); activating $G_{\alpha q}$ in the AWC is both necessary and sufficient for LTAM following one CS-US pairing. Moreover, $G_{\alpha q}$ signaling in the AWC slows cognitive decline and restores LTAM ability at an age when associative memory ability has been abrogated. Cell non-autonomous regulation of memory formation is not well understood; since long-term memory components and processes are highly conserved between *C. elegans* and higher organisms (Kauffman et al., 2010; Lakhina et al., 2015; Stein and Murphy, 2014), the molecules downstream of $G_{\alpha q}$ signaling may present new targets for the study of learning, memory, and aging in mammals. This cell non-autonomous regulation occurs via neuropeptide signaling (Figure 6), which has previously been implicated in *C. elegans* LTAM (Lakhina et al., 2015). Neuropeptides from the AWC likely activate signaling pathways upstream of CREB, such as CAMKII and JNK signaling, which potentially regulate CREB activity in a positive feed-forward loop during memory training (Lakhina et al., 2015), though a number of other signaling pathways could be involved.

We also found that increasing $G_{\alpha q}$ signaling in the AWC alone dissociates the positive influence of this pathway on memory formation from its previously-reported deleterious effects on lifespan (Ch’ng et al., 2008). Our elucidation of the neural site where $G_{\alpha q}$ signaling regulates memory may enable the identification of molecules that promote memory maintenance without shortening lifespan. These could represent targets for novel

strategies to manipulate memory consolidation, and may potentially provide new therapeutics that treat cognitive decline or prevent deleterious consolidation.

STAR Methods

CONTACT FOR REAGENT AND RESOURCE SHARING

Further information and requests for resources and reagents should be directed to and will be fulfilled by the Lead Contact, Coleen Murphy (ctmurphy@princeton.edu).

EXPERIMENTAL MODEL AND SUBJECT DETAILS

C. elegans genetics—All strains were maintained at 20°C on plates made from standard nematode growth medium (NGM: 3 g/L NaCl, 2.5 g/L Bacto-peptone, 17 g/L Bacto-agar in distilled water, with 1mL/L cholesterol (5 mg/mL in ethanol), 1 mL/L 1M $CaCl_2$, 1 mL/L 1M $MgSO_4$, and 25 mL/L 1M potassium phosphate buffer (pH 6.0) added to molten agar after autoclaving; (Brenner, 1974) or high growth medium (HGM: NGM recipe modified as follows: 20 g/L Bacto-peptone, 30 g/L Bacto-agar, and 4mL/L cholesterol (5 mg/mL in ethanol); all other components same as NGM), with OP50 E. coli as the food source. Experiments that did not involve RNAi treatments were performed using NGM plates seeded with OP50 E. coli for *ad libitum* feeding (Brenner, 1974); for RNAi experiments, the standard NGM molten agar was supplemented with 1 mL/L 1M IPTG (isopropyl β-d-1-thiogalactopyranoside) and 1mL/L 100mg/mL carbenicillin, and plates were seeded with HT115 E. coli or OP50(xu3363) E. coli for *ad libitum* feeding. Hypochlorite-synchronization to developmentally synchronize experimental animals was performed by collecting eggs from gravid hermaphrodites via exposure to an alkaline-bleach solution (*e.g.*, 5.5 mL water, 1.5 mL 5N KOH, 3.0 mL sodium hypochlorite), followed by repeated washing of collected eggs in M9 buffer (6 g/L Na_2HPO_4, 3 g/L KH_2PO_4, 5 g/L NaCl and 1 mL/L 1M $MgSO_4$ in distilled water; (Brenner, 1974)). For aging experiments, animals were transferred at the L4 larval stage onto NGM plates supplemented with 500μl/L 0.1M FUdR (5-Fluoro-2′-deoxyuridine) for a final concentration of 0.05M FUdR.

Strains: Wild-type: (N2 Bristol); Mutant strains: NM1380 *(egl-30(js126)),* OH161 (*ttx-3(ot22)),* RB816 (*sra-11(ok630)),* UTK2 (*mbr-1(qa5901)),* MT1434 (*egl-30(n686)),* MT1083 (*egl-8(n488)),* KG1278 (*unc-63(ce362)),* YT17 (*crh-1(tz2)),* DG1856 (*goa-1(sa734)),* and KP2342 (*pkc-1(nu488))* were obtained from the *Caenorhabditis* Genetics Center (University of Minnesota, Minneapolis, MN). The AIM CREB Rescue CQ159 (*crh-1(tz2); wqEx29 [Pmyo-2::mCherry]/PuroR; Pmbr-1::crh-1β::FLAG)* and SIA CREB Rescue CQ160 (*crh-1(tz2); wqEx29 [Pmyo-2::mCherry]/PuroR; Pceh-24::crh-1β::FLAG),* and CQ161 (*pCRE::GFP)* lines were described previously (Lakhina et al., 2015; Suo et al., 2006). Strains JN897 (*Podr-1::egl-30(Q205L))* and JN819 (*Podr-1::goa-1(Q205L))* were kind gifts from Y. Iino (University of Tokyo, Tokyo, Japan), IV183 (*ueEx104 [odr-3::unc-31sense::sl2mCherry, odr-3::unc-31antisense::sl2mCherry, unc-122::RFP])* and IV8 (*ueEx4 [odr-3::eat-4 sense, odr-3::eat-4 antisense, eat-2::GFP])* were gifts from S. Chalasani (The Salk Institute for Biological Studies, La Jolla, CA), and CX9735 (*gcy-28(tm2411);kyEX2139[odr-3::pkc1(A160E)::sl2GFP, elt-2::GFP])* was a generous gift from C. Bargmann (The Rockefeller University, New York, NY).

The following strains were generated by crosses: CQ210 ((*egl-30(js126); crh-1(tz2)*) was generated by crossing NM1380 *(egl-30(js126))* with YT17 (*crh-1(tz2)),* CQ243 (*egl-30(js126); crh-1(tz2);wqEx29 [Pmyo-2::mCherry]/PuroR;Pceh-24::crh-1β::FLAG)* was generated by crossing CQ210 ((*egl-30(js126); crh-1(tz2*)) with SIA CREB Rescue CQ160 (*crh-1(tz2);wqEx29 [Pmyo-2::mCherry]/PuroR;Pceh-24::crh-1β::FLAG)*, CQ245 *(egl-30(js126); crh-1(tz2);wqEx29 [Pmyo-2::mCherry]/PuroR;Pmbr-1::crh-1β::FLAG)* was generated by crossing CQ210 (*(egl-30(js126); crh-1(tz2))* with AIM CREB Rescue CQ159 (*crh-1(tz2);wqEx29[Pmyo-2::mCherry]/PuroR;Pmbr-1::crh-1β::FLAG),* CQ252 *(egl-30(js126);wqEx28[pCRE::GFP])* was generated by crossing NM1380 *(egl-30(js126))* with CQ161 (*pCRE::GFP),* CQ253 *(egl-30(js126);Podr-1::goa-1(Q205L))* was generated by crossing NM1380 *(egl-30(js126))* with JN819 (*Podr-1::goa-1(Q205L)),* CQ294 (*egl-8(n488);Podr-1::egl-30(Q205L))* was generated by crossing JN897 (*Podr-1::egl-30(Q205L))* with MT1083 (*egl-8(n488)),* CQ406 *(mbr-1(qa5901);Podr-1::egl-30(Q205L))* was generated by crossing JN897 (*Podr-1::egl-30(Q205L))* with UTK2 (*mbr-1(qa5901)),* CQ407 *(egl-30(js126);ueEx104[odr-3::unc-31sense::sl2mCherry,odr-3::unc-31antisense::sl2mCherry,unc-122::RFP])* was generated by crossing NM1380 *(egl-30(js126))* with IV183 (*ueEx104[odr-3::unc-31sense::sl2mCherry,odr-3::unc-31antisense::sl2mCherry,unc-122::RFP]),* CQ412 (*egl-30(js126);ueEx4[odr-3::eat-4 sense, odr-3::eat-4 antisense,eat-2::GFP)* was generated by crossing NM1380 *(egl-30(js126))* with IV8 (*ueEx4[odr-3::eat-4 sense, odr-3::eat-4 antisense, eat-2::GFP]),* CQ415 *(crh-1(tz2);Podr-1::egl-30(Q205L))* was generated by crossing JN897 (*Podr-1::egl-30(Q205L))* with YT17 (*crh-1(tz2))*, CQ465 *(ttx-3(ot22);Podr-1::egl-30(Q205L))* was generated by crossing JN897 (*Podr-1::egl-30(Q205L))* with OH161 (*ttx-3(ot22)),* CQ547 (*Podr-1::egl-30(V180M);pCRE::GFP))* was generated by crossing CQ477 *(Podr-1::egl-30(V180M))* with CQ161 (*pCRE::GFP),* CQ563 (*Podr-3::pkc1(A160E)::sl2GFP, elt-2::GFP*) was generated by crossing CX9735 (*gcy-28(tm2411);kyEX2139[Podr-3::pkc1(A160E)::sl2GFP, elt-2::GFP])* with N2 (Bristol) and selecting heterozygotes for self-fertilization, followed by genotyping of F1 progeny for to isolate N2 animals that expressed *kyEX2139[odr-3::pkc1(A160E)::sl2GFP, elt-2::GFP].*

Construction of Transgenic Lines: Extrachromosomal transgenic arrays were generated as previously describe (Mello et al., 1991). For CQ477 *(Podr-1::egl-30(V180M))*, the *egl-30* gene (bearing the V180M mutation) was PCR amplified from *egl-30(js126)* mutants. The *egl-30(V180M)* was PCR ligated to 2400bp upstream of the *odr-1* start site and the *unc-54* 3′UTR. *Podr-1::egl-30(V180M)* was injected into animals at 15ng/μl with 1 ng/μl *Pmyo-2::mcherry.* The *HS Inducible Podr-1::egl-30(Q205L)* lines CQ429 (*pHSP16–48::FLPase; Podr-1::FRT::egl-30(Q205L); Pmyo-2::mCherry)* and CQ430 (*pHSP16–48::FLPase; Podr-1::FRT::egl-30(Q205L); Pmyo-2::mCherry) #2* were constructed as described previously (Davis et al., 2008). FLP cloning plasmids were a gift of E. Jorgensen. Briefly, the upstream 2.4kb promoter of *odr-1* was used to drive expression of a FRT-flanked mCherry expression cassette, followed by GFP N-terminally fused to *egl-30(Q205L)* and the *unc-54* 3′UTR. N2 worms were injected with 25 ng/ul of the inducible *odr-1p::FRT-mCherry-FRT::GFP-egl-30(Q205L)* plasmid, 45 ng/ul of *hsp16.48p::FLPase*, and 1 ng/μl *Pmyo-2::mcherry.*

METHOD DETAILS

Behavioral Assays

Olfactory associative paradigms: Wild-type, mutant, and transgenic animals were trained and tested for either long-term or short/intermediate term memory as previously described (Kauffman et al., 2010). Briefly, synchronized day 1 adult hermaphrodites were washed from HGM of NGM plates with M9 buffer, allowed to settle by gravity, and washed again with M9 buffer. After washing, the animals are starved for 1 hr in M9 buffer. For 1 CS-US pairing, worms were then transferred to 10 cm NGM conditioning plates (seeded with OP50 *E. coli* bacteria and with 6μl 10% 2-butanone (Acros Organics) in ethanol on the lid) for 1 hr. For 7 CS-US pairings, worms alternate between 30 minute conditioning cycles and 30 minute starvation cycles (on NGM plates with no food). After conditioning, the trained population of worms were tested for chemotaxis to 10% butanone vs. an ethanol control either immediately (0 hr) or after being transferred to 10 cm NGM plates with fresh OP50 for specified intervals before testing (30 mins-48 hrs), using standard, previously described chemotaxis assay conditions (Bargmann et al., 1993).

Chemotaxis indices were calculated as follows: $\mathbf{(\#worms_{Butanone} - \#worms_{Ethanol})/(Total\ \#worms)}$. Performance index is the change in chemotaxis index following training relative to the naïve chemotaxis index. The calculation for Performance Index is: $\mathbf{Chemotaxis\ Index_{Trained} - Chemotaxis\ Index_{Naive}}$. Performance indices for extrachromosomal transgenic strains (including strains that expressed AWC-specific RNAi) were analyzed by hand counting GFP or mCherry positive and negative worms at different locations on the chemotaxis plates. Wild-type controls for these experiments were the transgenic worms' GFP or mCherry negative siblings.

Assays using Drug Treatments: 100 μg/mL Actinomycin D ≥ 95% (Sigma Aldrich, Saint Louis, Missouri) was added to M9 buffer for the 1 hour pre-conditioning starvation and added to S-basal (5.8g/L NaCl, 50mL/L 1M potassium phosphate buffer (pH 6.0), and 5 mL/L cholesterol (5 mg/mL in ethanol)) during conditioning along with 1:1000 Butanone and OP50 *E. coli* bacteria that had been grown overnight. After treatment, worms were transferred to NGM plates seeded with OP50 *E. coli* until memory was assessed 24 hours postconditioning. To verify that Actinomycin D treatment blocked transcription, a separate cohort of animals were exposed to heat shock at 33°C while in M9 buffer or 100 μg/mL Actinomycin D in M9 followed by RNA isolation and qPCR to measure *hsp-70* gene expression. Cycloheximide ≥ 94% (Sigma Aldrich, Saint Louis, Missouri) was added to NGM at 0.8 mg/mL. Plates were poured and solidified overnight at 4°C, then seeded with OP50 *E. coli*. Animals were exposed to cycloheximide during conditioning and for 1 hour post-conditioning, after which they were transferred to NGM plates seeded with OP50 *E. coli* until long-term memory was assessed 24 hours post-conditioning.

RNA Collection and Microarray Hybridization—Worms of a particular genotype were crushed in liquid nitrogen and added to Trizol (Thermo Fisher Scientific). RNA was extracted and purified using an RNeasy Mini Kit (Qiagen, Germantown, MD, USA), cRNA was linearly amplified and Cy3/Cy5 labeled (Agilent, Santa Clara, CA, USA), and hybridized to Agilent 44k *C. elegans* microarrays, at 60°C overnight, as previously desc

ribed (Shaw et al., 2007). Three biological replicates of *egl-30(js126)* versus wild-type N2 arrays were hybridized to determine expression profiles of CREB-dependent, training dependent genes that had been previously identified (Lakhina et al., 2015).

Microarray analysis—Data from scanned microarrays were loaded onto the Princeton University MicroArray database (PUMAdb) (http://puma.princeton.edu), and analyzed as previously described (Shaw et al., 2007). Genes were filtered for presence in at least 60% of arrays (uncentered correlation, average linking). Log2 expression ratios of "CREB/LTAM" genes were hierarchically clustered after filtering for genes that were present in at least 60% of the arrays (uncentered correlation, average linking) in Cluster and displayed in TreeView (Eisen et al., 1998).

RNA Isolation, CDNA synthesis and qRT-PCR—Worms of a particular genotype were crushed in liquid nitrogen and added to Trizol reagent (Thermo Fisher Scientific). RNA was isolated per manufacturer's instructions, followed by DNase treatment (Qiagen). cDNA was synthesized with an oligo dT primer and Superscript III reverse transcriptase enzyme (Thermo Fisher Scientific). cDNA was mixed with buffers, primers, SYBR green, and hot start Taq polymerase in a master mix prepared by a manufacturer (Thermo Fisher Scientific). Using a Real-Time PCR machine (7500 Real Time PCR machine, Applied Biosystems) PCR reactions were run followed by a dissociation reaction to determine specificity of the amplified product. The amount of gene expression was quantified using the ΔΔCt method using *pmp-3* as a reference gene. Primer sets are listed in the key reagents and resources table.

Microscopy—Z-stack multi-channel (DIC, GFP) of *pCRE::GFP* animals were imaged every 1 mm at 60X magnification; Maximum Intensity Projections and 3D reconstructions of head neurons were built with Nikon *NIS-Elements*. To quantify *pCRE::GFP* levels worms were synchronized by bleaching, and eggs were plated on OP50-seeded NGM plates until Day 1 of adulthood. For imaging at Day 5 of adulthood, animals were transferred to OP50-seeded NGM plates containing 0.05 mM FUdR to prevent progeny contamination. GFP was imaged at 60X magnification and quantified using *NIS-Elements* software. Average pixel intensity was measured over a standard region of interest (the AIM) in every animal.

Survival analysis—Lifespans were performed on *Podr-1::egl-30(Q205L)* and *Podr-1::egl-30(V180M)* transgenic animals and their wild-type siblings bleached on to OP50 seeded NGM plates. At the L4 Larval stage, transgenic worms (expressing GFP or mCherry) or non-fluorescent wild-type siblings, were picked for survival analysis. Worms were transferred every other day to freshly seeded plates. Day 1 of adulthood was defined as t=0, and the log-rank (Mantel-Cox) method was used to test the null hypothesis in Kaplan-Meier survival analysis, and evaluated using OASIS survival analysis software (Yang et al., 2011). All experiments were carried out at 20°C; N = 108 per s train/trial. Two biological replicates were performed.

QUANTIFICATION AND STATISTICAL ANALYSIS

Lifespan assays were assessed using Kaplan-Meier log rank tests. For the comparison of performance indices between two genotypes (i.e. *egl-30js126* vs wild-type), two-tailed unpaired Student's t-tests with Welch's corrections were used. For the comparison of relative fluorescence between two genotypes (i.e. *egl-30js126* vs wild-type), two-tailed unpaired Student's t-tests with Welch's corrections were used. When relative fluorescence was measured across timepoints (0hr, 1hr, 2hr, 4hr, 6hr), one-way analysis of variances followed by Bonferroni post hoc tests for multiple comparisons were performed. 2-way ANOVAs were used for evaluating effects between genotype (*egl-30(js126)* and wild-type) and timepoint (0hr, 4hr, 24hr) on chemotaxis and performance indices with a significant interaction between factors ($p < 0.0001$) leading to the performance of Bonferroni post-hoc comparisons to determine differences between individual groups. Experiments were repeated on separate days with separate populations, to confirm that results were reproducible. Prism 7 software was used for all statistical analyses; software and further statistical details used for microarray analyses are described in the method details section of the STAR methods. Additional statistical details of experiments, including sample size (with n representing the number of chemotaxis assays performed for behavior, RNA collections for qPCR and arrays, and number of worms for microscopy), can be found in the figure legends.

DATA AND SOFTWARE AVAILABILITY

Raw microarray datasets are publically available through PUMAdb (http://puma.princeton.edu). For this publication, refer to https://puma.princeton.edu/cgi-bin/publication/viewPublication.pl?pub_no=582.

Supplementary Material

Refer to Web version on PubMed Central for supplementary material.

Acknowledgments

We thank J. Ashraf for assistance with the generation of transgenic strains, M. Wright and R. Jin for assistance in behavioral assays, the CGC for strains, and the Murphy lab for valuable discussion. FLP cloning plasmids were a gift from E. Jorgensen. Strains JN897 and JN819 were kind gifts from Y. Iino, IV183 and IV8 were generously provided by S. Chalasani, and CX9735 was a kind gift from C. Bargmann. CTM is the Director of the Paul F. Glenn Center for Biology of Aging Research at Princeton and an HHMI-Simons Faculty Scholar. This work was supported by the NIH (Cognitive Aging R01) to CTM and an F32 NRSA to RNA.

References

Abeliovich A, Paylor R, Chen C, Kim JJ, Wehner JM, Tonegawa S. PKC gamma mutant mice exhibit mild deficits in spatial and contextual learning. Cell. 1993; 75:1263–1271. [PubMed: 8269510]

Adachi T, Kunitomo H, Tomioka M, Ohno H, Okochi Y, Mori I, Iino Y. Reversal of salt preference is directed by the insulin/PI3K and Gq/PKC signaling in Caenorhabditis elegans. Genetics. 2010; 186:1309–1319. [PubMed: 20837997]

Arey RN, Murphy CT. Conserved regulators of cognitive aging: From worms to humans. Behav Brain Res. 2017; 322:299–310. [PubMed: 27329151]

Bargmann CI, Hartwieg E, Horvitz HR. Odorant-selective genes and neurons mediate olfaction in C. elegans. Cell. 1993; 74:515–527. [PubMed: 8348618]

Bilkei-Gorzo A, Albayram O, Draffehn A, Michel K, Piyanova A, Oppenheimer H, Dvir-Ginzberg M, Rácz I, Ulas T, Imbeault S, et al. A chronic low dose of Δ(9)-tetrahydrocannabinol (THC) restores cognitive function in old mice. Nat Med. 2017; 23:782–787. [PubMed: 28481360]

Brenner S. The genetics of Caenorhabditis elegans. Genetics. 1974; 77:71–94. [PubMed: 4366476]

Brundage L, Avery L, Katz A, Kim UJ, Mendel JE, Sternberg PW, Simon MI. Mutations in a C. elegans Gqalpha gene disrupt movement, egg laying, and viability. Neuron. 1996; 16:999–1009. [PubMed: 8630258]

Burke SN, Barnes CA. Neural plasticity in the ageing brain. Nat Rev Neurosci. 2006; 7:30–40. [PubMed: 16371948]

Ch'ng Q, Sieburth D, Kaplan JM. Profiling synaptic proteins identifies regulators of insulin secretion and lifespan. PLoS Genet. 2008; 4:e1000283. [PubMed: 19043554]

Chen BL, Hall DH, Chklovskii DB. Wiring optimization can relate neuronal structure and function. Proc Natl Acad Sci U S A. 2006; 103:4723–4728. [PubMed: 16537428]

Davis MW, Morton JJ, Carroll D, Jorgensen EM. Gene activation using FLP recombinase in C. elegans. PLoS Genet. 2008; 4:e1000028. [PubMed: 18369447]

Dekker LV, McIntyre P, Parker PJ. Mutagenesis of the regulatory domain of rat protein kinase C-eta. A molecular basis for restricted histone kinase activity. J Biol Chem. 1993; 268:19498–19504. [PubMed: 8396139]

Eisen MB, Spellman PT, Brown PO, Botstein D. Cluster analysis and display of genome-wide expression patterns. Proc Natl Acad Sci U S A. 1998; 95:14863–14868. [PubMed: 9843981]

Frederick AL, Saborido TP, Stanwood GD. Neurobehavioral phenotyping of G(αq) knockout mice reveals impairments in motor functions and spatial working memory without changes in anxiety or behavioral despair. Front Behav Neurosci. 2012; 6:29. [PubMed: 22723772]

Fusco S, Ripoli C, Podda MV, Ranieri SC, Leone L, Toietta G, McBurney MW, Schütz G, Riccio A, Grassi C, et al. A role for neuronal cAMP responsive-element binding (CREB)-1 in brain responses to calorie restriction. Proc Natl Acad Sci U S A. 2012; 109:621–626. [PubMed: 22190495]

Hawasli AH, Saifee O, Liu C, Nonet ML, Crowder CM. Resistance to volatile anesthetics by mutations enhancing excitatory neurotransmitter release in Caenorhabditis elegans. Genetics. 2004; 168:831–843. [PubMed: 15514057]

Josselyn SA, Shi C, Carlezon WA, Neve RL, Nestler EJ, Davis M. Long-term memory is facilitated by cAMP response element-binding protein overexpression in the amygdala. J Neurosci. 2001; 21:2404–2412. [PubMed: 11264314]

Kaletsky R, Lakhina V, Arey R, Williams A, Landis J, Ashraf J, Murphy CT. The C. elegans adult neuronal IIS/FOXO transcriptome reveals adult phenotype regulators. Nature. 2016; 529:92–96. [PubMed: 26675724]

Kauffman AL, Ashraf JM, Corces-Zimmerman MR, Landis JN, Murphy CT. Insulin signaling and dietary restriction differentially influence the decline of learning and memory with age. PLoS Biol. 2010; 8:e1000372. [PubMed: 20502519]

Kim SW, Seo M, Kim DS, Kang M, Kim YS, Koh HY, Shin HS. Knockdown of phospholipase C-β1 in the medial prefrontal cortex of male mice impairs working memory among multiple schizophrenia endophenotypes. J Psychiatry Neurosci. 2015; 40:78–88. [PubMed: 25268789]

Kudo K, Wati H, Qiao C, Arita J, Kanba S. Age-related disturbance of memory and CREB phosphorylation in CA1 area of hippocampus of rats. Brain Res. 2005; 1054:30–37. [PubMed: 16054117]

Lackner MR, Nurrish SJ, Kaplan JM. Facilitation of synaptic transmission by EGL-30 Gqalpha and EGL-8 PLCbeta: DAG binding to UNC-13 is required to stimulate acetylcholine release. Neuron. 1999; 24:335–346. [PubMed: 10571228]

Lakhina V, Arey RN, Kaletsky R, Kauffman A, Stein G, Keyes W, Xu D, Murphy CT. Genome-wide functional analysis of CREB/long-term memory-dependent transcription reveals distinct basal and memory gene expression programs. Neuron. 2015; 85:330–345. [PubMed: 25611510]

Leinwand SG, Chalasani SH. Neuropeptide signaling remodels chemosensory circuit composition in Caenorhabditis elegans. Nat Neurosci. 2013; 16:1461–1467. [PubMed: 24013594]

Lenart A, Vaupel JW. Questionable evidence for a limit to human lifespan. Nature. 2017; 546:E13–E14. [PubMed: 28658239]

Li LB, Lei H, Arey RN, Li P, Liu J, Murphy CT, Xu XZ, Shen K. The Neuronal Kinesin UNC-104/KIF1A Is a Key Regulator of Synaptic Aging and Insulin Signaling-Regulated Memory. Curr Biol. 2016

Matsuki M, Kunitomo H, Iino Y. Goalpha regulates olfactory adaptation by antagonizing Gqalpha-DAG signaling in Caenorhabditis elegans. Proc Natl Acad Sci U S A. 2006; 103:1112–1117. [PubMed: 16418272]

Mello CC, Kramer JM, Stinchcomb D, Ambros V. Efficient gene transfer in C.elegans: extrachromosomal maintenance and integration of transforming sequences. EMBO J. 1991; 10:3959–3970. [PubMed: 1935914]

Miller KG, Emerson MD, Rand JB. Goalpha and diacylglycerol kinase negatively regulate the Gqalpha pathway in C. elegans. Neuron. 1999; 24:323–333. [PubMed: 10571227]

Park DC, Lautenschlager G, Hedden T, Davidson NS, Smith AD, Smith PK. Models of visuospatial and verbal memory across the adult life span. Psychol Aging. 2002; 17:299–320. [PubMed: 12061414]

Sacktor TC, Hell JW. The genetics of PKMζ and memory maintenance. Sci Signal. 2017:10.

Sekeres MJ, Mercaldo V, Richards B, Sargin D, Mahadevan V, Woodin MA, Frankland PW, Josselyn SA. Increasing CRTC1 function in the dentate gyrus during memory formation or reactivation increases memory strength without compromising memory quality. J Neurosci. 2012; 32:17857–17868. [PubMed: 23223304]

Shaw WM, Luo S, Landis J, Ashraf J, Murphy CT. The C. elegans TGF-beta Dauer pathway regulates longevity via insulin signaling. Curr Biol. 2007; 17:1635–1645. [PubMed: 17900898]

Shen Y, Zhang J, Calarco JA, Zhang Y. EOL-1, the homolog of the mammalian Dom3Z, regulates olfactory learning in C. elegans. J Neurosci. 2014; 34:13364–13370. [PubMed: 25274815]

Sieburth D, Madison JM, Kaplan JM. PKC-1 regulates secretion of neuropeptides. Nat Neurosci. 2007; 10:49–57. [PubMed: 17128266]

Silva AJ, Kogan JH, Frankland PW, Kida S. CREB and memory. Annu Rev Neurosci. 1998; 21:127–148. [PubMed: 9530494]

Stein GM, Murphy CT. C. elegans positive olfactory associative memory is a molecularly conserved behavioral paradigm. Neurobiol Learn Mem. 2014; 115:86–94. [PubMed: 25108196]

Sun MK, Alkon DL. The “memory kinases”: roles of PKC isoforms in signal processing and memory formation. Prog Mol Biol Transl Sci. 2014; 122:31–59. [PubMed: 24484697]

Suo S, Kimura Y, Van Tol HH. Starvation induces cAMP response element-binding protein-dependent gene expression through octopamine-Gq signaling in Caenorhabditis elegans. J Neurosci. 2006; 26:10082–10090. [PubMed: 17021164]

Sutton MA, Bagnall MW, Sharma SK, Shobe J, Carew TJ. Intermediate-term memory for site-specific sensitization in aplysia is maintained by persistent activation of protein kinase C. J Neurosci. 2004; 24:3600–3609. [PubMed: 15071108]

Tsunozaki M, Chalasani SH, Bargmann CI. A behavioral switch: cGMP and PKC signaling in olfactory neurons reverses odor preference in C. elegans. Neuron. 2008; 59:959–971. [PubMed: 18817734]

Villeda SA, Plambeck KE, Middeldorp J, Castellano JM, Mosher KI, Luo J, Smith LK, Bieri G, Lin K, Berdnik D, et al. Young blood reverses age-related impairments in cognitive function and synaptic plasticity in mice. Nat Med. 2014; 20:659–663. [PubMed: 24793238]

Vukojevic V, Gschwind L, Vogler C, Demougin P, de Quervain DJ, Papassotiropoulos A, Stetak A. A role for α-adducin (ADD-1) in nematode and human memory. EMBO J. 2012; 31:1453–1466. [PubMed: 22307086]

Weeber EJ, Atkins CM, Selcher JC, Varga AW, Mirnikjoo B, Paylor R, Leitges M, Sweatt JD. A role for the beta isoform of protein kinase C in fear conditioning. J Neurosci. 2000; 20:5906–5914. [PubMed: 10934237]

Yang JS, Nam HJ, Seo M, Han SK, Choi Y, Nam HG, Lee SJ, Kim S. OASIS: online application for the survival analysis of lifespan assays performed in aging research. PLoS One. 2011; 6:e23525. [PubMed: 21858155]

Yin JC, Del Vecchio M, Zhou H, Tully T. CREB as a memory modulator: induced expression of a dCREB2 activator isoform enhances long-term memory in Drosophila. Cell. 1995; 81:107–115. [PubMed: 7720066]

Yu XW, Curlik DM, Oh MM, Yin JC, Disterhoft JF. CREB overexpression in dorsal CA1 ameliorates long-term memory deficits in aged rats. Elife. 2017:6.

Zong W, Liu S, Wang X, Zhang J, Zhang T, Liu Z, Wang D, Zhang A, Zhu M, Gao J. Trio gene is required for mouse learning ability. Brain Res. 2015; 1608:82–90. [PubMed: 25727174]

Highlights

- Increased $G_{\alpha q}$ signaling enhances memory and slows age-related cognitive decline
- CREB activity underlies enhanced consolidation and memory maintenance with age
- The AWC neuron is the site where $G_{\alpha q}$ signaling regulates memory
- $G_{\alpha q}$ activation in the AWC of aged animals rescues cognitive decline

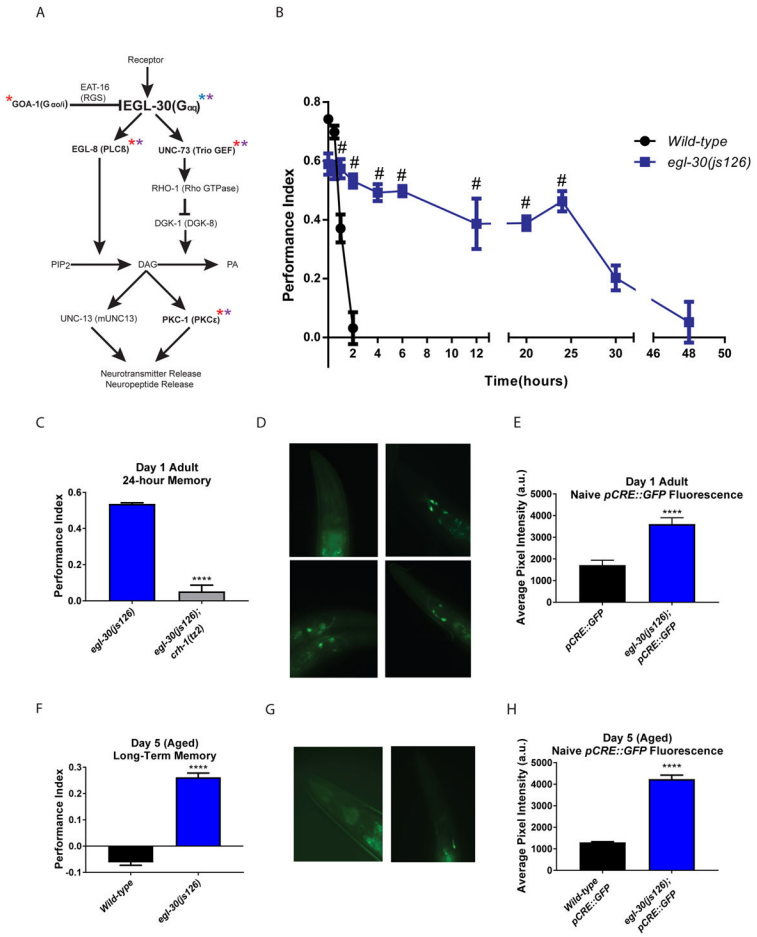

Figure 1. Activation of $G_{\alpha q}$ enhances consolidation and prevents age-related decline in memory performance via increased CREB activity

A) Diagram of $G_{\alpha q}$ pathway. Animals bearing hypomorphic mutations in components of this signaling pathway are defective for normal associative learning and memory (indicated by *). * = Defect in learning after 1 CS-US pairing, * = Defect in short-term memory, * = Defect in learning after 7 CS-US pairings. For performance indices, see Figure S1. **B)** Day 1 adult animals with a gain-of-function (*js126*) mutation in *egl-30* exhibit extended memory (~24–30 hrs) following 1 CS-US pairing when compared to the memory of wild-type animals (~2hrs). Mean ± SEM. n ≥ 9–12 per timepoint. #p<0.0001 when compared to wild-type animals at same timepoint (data not shown). **C)** *egl-30(js126)* animals lacking functional CREB [*egl-30(js126);crh-1(tz2)*] do not display extended memory, indicating the extended memory is LTAM (CREB-dependent). Mean ± SEM. n ≥ 24–26 per genotype. ****p<0.0001. **D)** CREB activity is elevated in AIM/SIA of naive *egl-30(js126);pCRE::GFP* animals, while GFP is undetectable in naïve wild-type *pCRE::GFP* animals. CREB activity is increased immediately following LTAM (7x) training in wild-type animals, while there is no observable increase in CREB activity following training (1x) in *egl-30(js126);pCRE::GFP* animals. **E)** Quantification of naïve wild-type *pCRE::GFP* vs. naïve *egl-30(js126);pCRE::GFP*. Mean ± SEM. n > 30 animals per genotype. ****p<0.0001. **F)** *egl-30(js126)* animals maintain the ability to form a long-term

memory after 1 CS-US pairing at Day 5 of adulthood. Mean ± SEM. n ≥ 10 per genotype. ****p<0.0001. **G)** Naïve (untrained) *egl-30(js126)* animals maintain elevated CREB activity in the AIM at Day 5 of adulthood, while wild-type worms lack AIM GFP. **H)** Quantification of naïve wild-type *pCRE::GFP* vs naïve *egl-30(js126);pCRE::GFP* on Day 5. Mean ± SEM. n > 26 animals per genotype. ****p<0.0001. See also Figure S1 and S2.

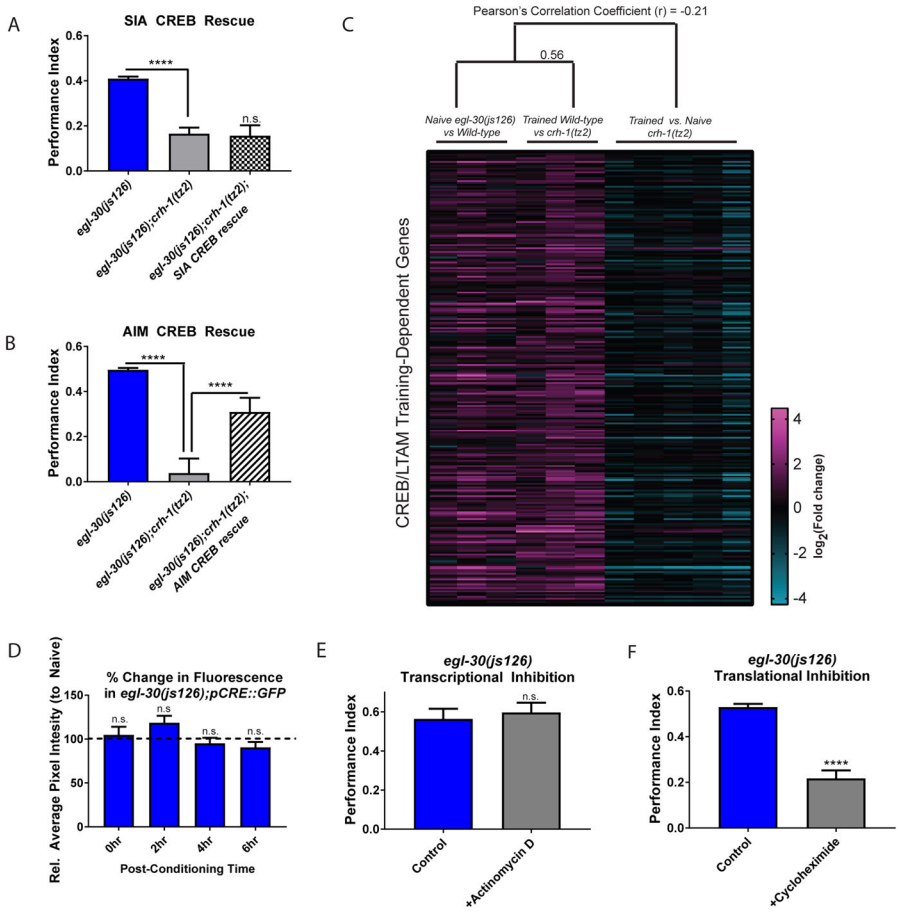

Figure 2. Increased CREB activity in the AIM neurons decreases the threshold for consolidation in animals with enhanced $G_{\alpha q}$ signaling by increasing transcription of "memory genes"

A) Rescue of CREB in the SIA fails to restore memory formation to *egl-30(js126);crh-1(tz2)* animals, while (**B**) CREB rescue in the AIM restores memory performance to a level comparable to *egl-30(js126)* animals. Mean ± SEM. n ≥ 11–12 per genotype. ****p<0.0001, n.s.= p>0.05. **C)** Expression of previously identified "CREB/LTAM dependent genes" (Lakhina et al., 2015), which are upregulated in wild-type animals following LTAM training in a CREB-dependent manner (middle) but remain unchanged following LTAM training in *crh-1(tz2)* mutants (right), are elevated in naïve *egl-30(js126)* animals (left). Expression of these genes in naïve *egl-30(js126)* animals correlates with their expression LTAM-trained wild-type animals (Pearson correlation = 0.56), and is anti-correlated with *crh-1(tz2)* mutants after LTAM training (−0.21). Individual columns represent the expression of "CREB/LTAM genes" for a single microarray. **D)** Quantification of *egl-30(js126);pCRE::GFP* animals up to 6 hours after training shows that CREB activity does not significantly increase after conditioning relative to naïve *egl-30(js126);pCRE::GFP* animals. Mean ± SEM. n ≥ 25–40 per timepoint. n.s = p>0.05. **E)** Inhibiting transcription by administration of actinomycin D during the pre-conditioning starve and conditioning has no detectable effect on long-term memory in *egl-30(js126)* animals. Mean ± SEM. n ≥ 10 per treatment. n.s.= p>0.05. **F)** Inhibiting translation by treatment with cycloheximide during conditioning and 1 hr post-conditioning abolishes long-term memory without affecting

learning (See Figure S2F) in *egl-30(js126)* animals. Mean ± SEM. n ≥ 15 per treatment. ****p<0.0001. See also Figure S2.

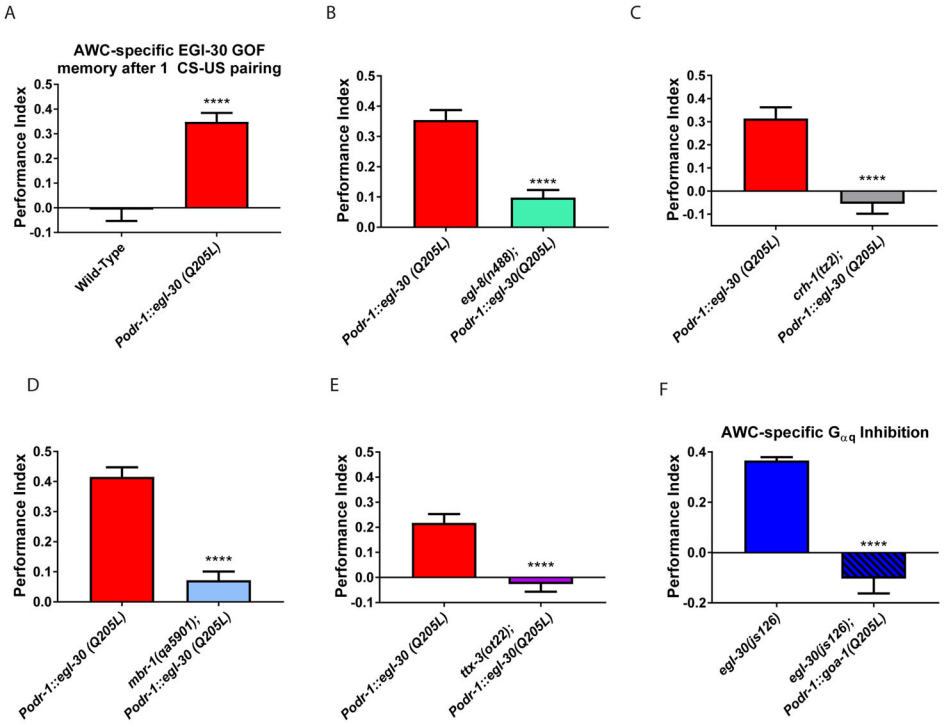

Figure 3. Activation of $G_{\alpha q}$ solely in the AWC is necessary and sufficient for long-term memory formation after 1 CS-US pairing

A) Expression of a gain-of-function EGL-30 (*Podr-1::egl-30(Q205L)*) in the AWC results in extended (24hr) memory following 1 CS-US pairing. Mean ± SEM. n ≥ 9 per genotype. ****p<0.0001. **B)** Extended memory of *Podr-1::egl-30(Q205L)* requires downstream $G_{\alpha q}$ signaling components, as *egl-8(n488);Podr-1::egl-30(Q205L)* animals do not display extended memory. Mean ± SEM. n ≥ 9–10 per genotype. ****p<0.0001. **C–E)** Extended memory in *Podr-1::egl-30(Q205L)* is CREB-dependent long-term memory. *Podr-1::egl-30(Q205L)* animals do not display extended memory without functional CREB (**C,** [*crh-1(tz2);Podr-1::egl-30(Q205L)*]), when AIM function is disrupted by an *mbr-1* mutation (**D,** [*mbr-1(qa5901);Podr-1::egl-30(Q205L)*]), or when AIA/AIY function is disrupted by a *ttx-3* mutation (**E,** [*ttx-3(ot22);Podr-1::egl-30(Q205L)*]). Mean ± SEM. n ≥ 9–15 per genotype. ****p<0.0001. **F)** Repressing EGL-30 activity in AWC of *egl-30(js126)* animals by AWC-specific expression of a gain-of-function inhibitor of $G_{\alpha q}$ signaling (*egl-30(js126);Podr-1::goa-1(Q205L))* blocks the ability to form long-term memory. Mean ± SEM. n ≥ 9 per genotype. ****p<0.0001. See also Figure S3 and S4.

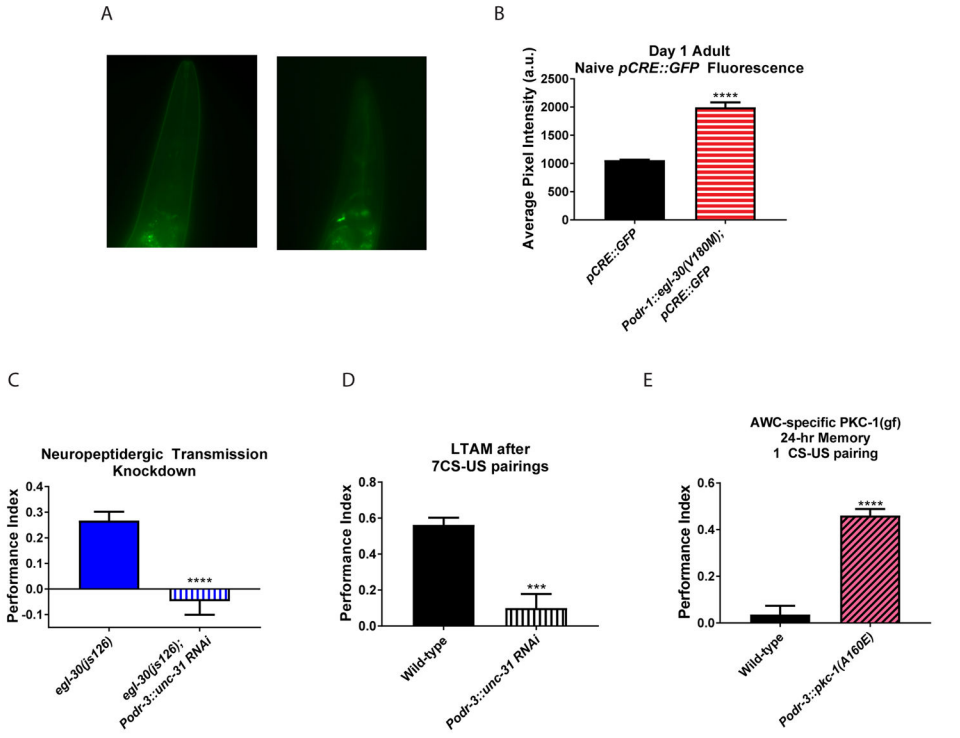

Figure 4. Enhanced $G_{\alpha q}$ signaling in the AWC cell non-autonomously regulates AIM CREB activity via neuropeptidergic signaling

A) CREB activity is elevated in the AIM of Day 1 adult naïve (untrained) *Podr-1::egl-30(V180M);pCRE::GFP* animals, which express an AWC-specific V180M *egl-30* gain-of-function allele of *egl-30* (allele present *egl-30(js126))*. **B)** Quantification of Day 1 naïve *Podr-1::egl-30(V180M);pCRE::GFP* vs naïve wild-type *pCRE::GFP.* Mean ± SEM. n > 30 animals per genotype. ****p<0.0001. **C)** Knockdown of neuropeptidergic signaling (*egl-30(js126);Podr-3::unc-31 RNAi))* from the AWC in *egl-30(js126)* animals abolishes the ability to form long-term memory after one CS-US pairing. Mean ± SEM. n ≥ 12 per genotype. ****p<0.0001. **D)** Neuropeptidergic signaling is necessary for normal long-term memory formation: knockdown of neuropeptidergic signaling (*Podr-3::unc-31 RNAi)* in the AWC of wild-type animals renders them unable to form long-term memory after 7 CS-US pairings. Mean ± SEM. n ≥ 9 per genotype. ****p<0.0001. **E)** Increasing neuropeptide secretion from the AWC via expression of a constitutively active PKC-1 (*Podr-3::pkc-1(A160E))* results in extended memory after 1 CS-US pairing. Mean ± SEM. n ≥ 10 per genotype. ****p<0.0001. See also Figure S4.

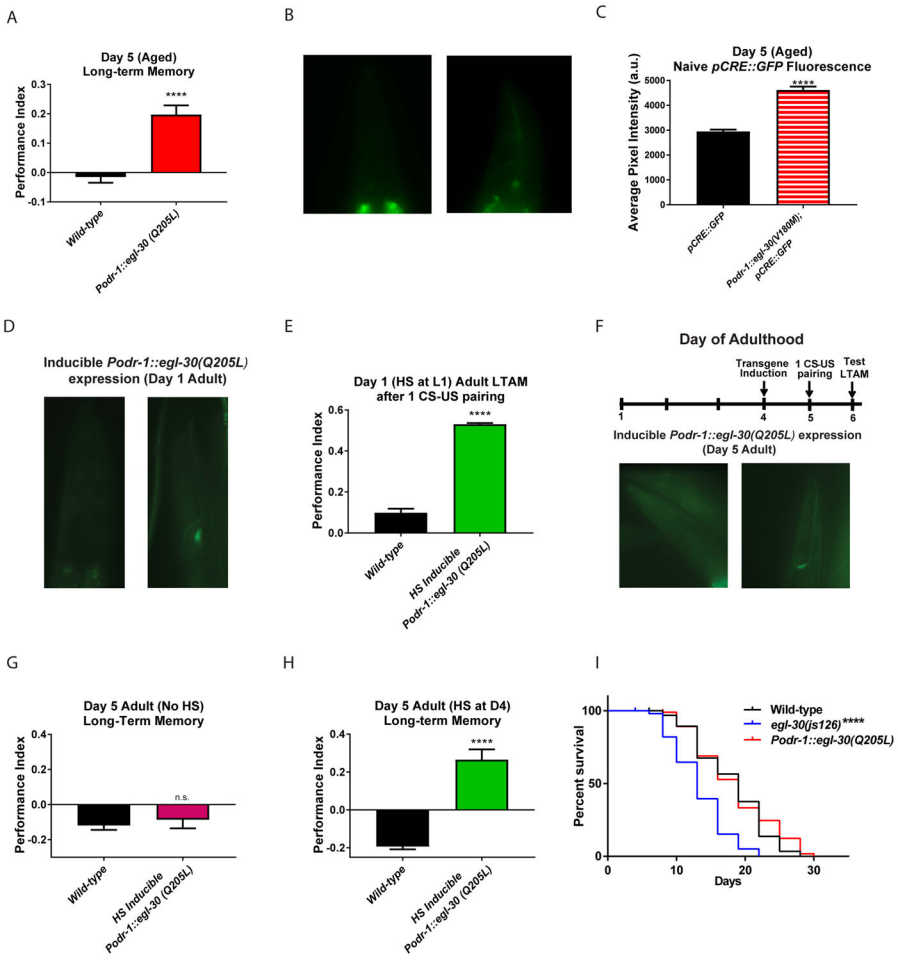

Figure 5. Activation of $G_{\alpha q}$ signaling solely in the AWC slows cognitive decline and restores cognitive function to aged animals

A) *Podr-1::egl-30(Q205L)* animals maintain the ability to form long-term memory after one CS-US pairing on Day 5 of adulthood. Mean ± SEM. n ≥ 13–14 per genotype. ****p<0.0001. **B)** Naïve (untrained) *Podr-1::egl-30(V180M);pCRE::GFP* animals maintain elevated CREB activity in the AIM on Day 5 of adulthood. **C)** Quantification of Day 5 naïve *Podr-1::egl-30(V180M);pCRE::GFP* vs naïve wild-type *pCRE::GFP.* Mean ± SEM. n > 40 animals per genotype. ****p<0.0001. **D)** 1 hour of heat shock (HS) at 34°C induces expression of a GFP-tagged gain-of-function EGL-30 in *HS Inducible Podr-1::egl-30(Q205L)* animals. **E)** Heat shock of *HS Inducible Podr-1::egl-30(Q205L)* animals at the L1 larval stage enables them to form long-term memories after one CS-US pairing at Day 1 of adulthood, while non-transgenic siblings are unaffected. Mean ± SEM. n ≥ 3 per genotype. ****p<0.0001. **F)** Schematic of induction of AWC-specific gain-of-function EGL-30 in aged animals. One hour of heat shock at 34°C on Day 4 of adulthood is sufficient to induce transgene expression that is detectable in Day 5 animals (1 hr HS). **G)** Animals without transgene induction (No HS) fail to form a long-term memory at Day 5 of adulthood. Mean ± SEM. n ≥ 4 per genotype. n.s = p>0.05. **H)** Induction of AWC-specific gain-of-function EGL-30 in aged (Day 4) animals enables long-term memory formation after one CS-US pairing on Day 5 of adulthood. Mean ± SEM. n ≥ 13 per genotype.

****p<0.0001. **I)** *egl-30(js126)* mutants have a significantly shortened lifespan (****p<0.0001), as previous reported (Ch'ng et al., 2008), while the lifespan of transgenic *Podr-1::egl-30(Q205L)* animals does not significantly differ from wild-type siblings (p = 0.47). n ≥ 100 per genotype. See also Figure S5.

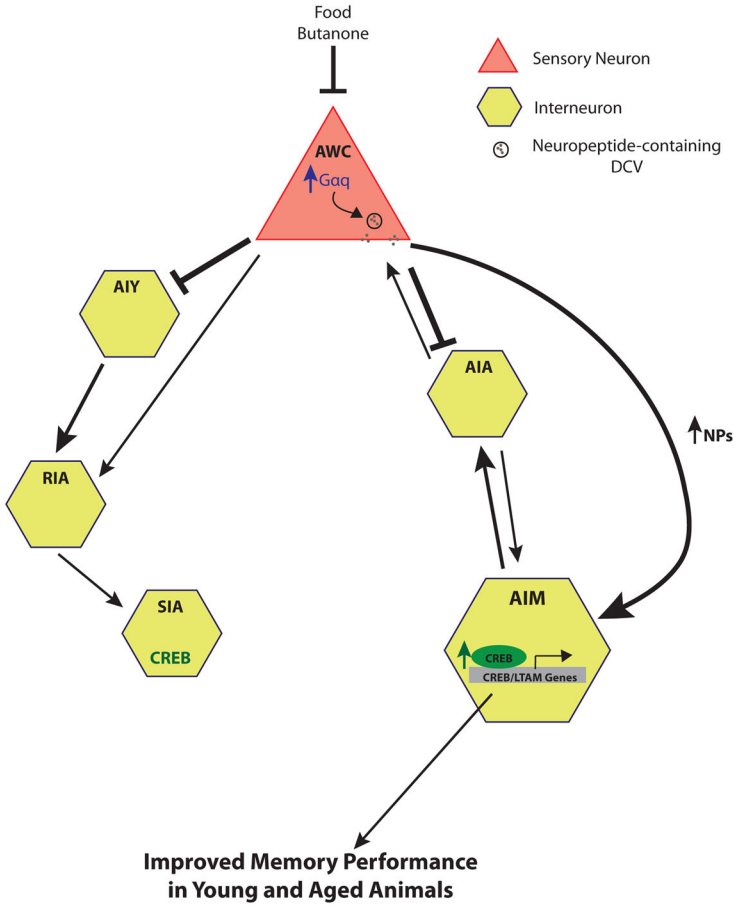

Figure 6. Model summarizing regulation of memory formation by increased $G_{\alpha q}$ signaling

Activation of $G_{\alpha q}$ signaling in the AWC increases the release of neuropeptides that signal to the downstream LTAM network, resulting in CREB activation in the AIM and enhanced memory performance.

KEY RESOURCES TABLE

REAGENT or RESOURCE	SOURCE	IDENTIFIER
Bacterial and Virus Strains		
E. coli: OP50	Caenorhabditis Genetics Center	OP50
E. coli: HT115	Caenorhabditis Genetics Center	HT115
Chemicals, Peptides, and Recombinant Proteins		
2-Butanone, 99+%, extra pure	Acros Organics	Cat# 149670250
Actinomycin D	Sigma-Aldrich	Cat# A4262
Cycloheximide	Sigma-Aldrich	Cat# C7698
Cyanine 3-CTP (Cy3)	PerkinElmer	Cat# NEL58000
Cyanine 5-CTP (Cy5)	PerkinElmer	Cat# NEL58100
TRIzol Reagent	Thermo Fisher Scientific	Cat# 15596026
Critical Commercial Assays		
Agilent Quick-Amp Labeling Kit, No Dye	Agilent	Cat# 5190-0447
RNeasy Mini Kit	Qiagen	Cat# 74104
Agilent Quick-Amp Labeling Kit, No Dye	Agilent	Cat# 5190-0447
Agilent Gene Expression Hybridization Kit	Agilent	Cat# 5188-5242
Power SYBR Green Master Mix	Thermo Fisher Scientific	Cat# 4367659
SuperScript III First Strand Synthesis System	Invitrogen	Cat# 18080-051
Deposited Data		
Raw microarray data	This Paper	PUMAdb (http://puma.princeton.edu).
Experimental Models: Organisms/Strains		
C. elegans strain N2 var. Bristol: wild-type	Caenorhabditis Genetics Center	N2
C. elegans strain NM1380: *egl-30(js126)*	Caenorhabditis Genetics Center	NM1380
C. elegans strain OH161: *ttx-3(ot22)*	Caenorhabditis Genetics Center	OH161
C. elegans strain RB816: *sra-11(ok630)*	Caenorhabditis Genetics Center	RB816
C. elegans strain MT1434: *egl-30(n686)*	Caenorhabditis Genetics Center	MT1434
C. elegans strain MT1083: *egl-8(n488)*	Caenorhabditis Genetics Center	MT1083
C. elegans strain KG1278: *unc-63(ce362)*	Caenorhabditis Genetics Center	KG1278
C. elegans strain YT17: *crh-1(tz2)*	Caenorhabditis Genetics Center	YT17
C. elegans strain DG1856: *goa-1(sa734)*	Caenorhabditis Genetics Center	DG1856
C. elegans strain KP2342: *pkc-1(nu488)*	Caenorhabditis Genetics Center	KP2342

REAGENT or RESOURCE	SOURCE	IDENTIFIER
C. elegans strain CQ159: *crh-1(tz2); wqEx29 [Pmyo-2::mCherry]/PuroR; Pmbr-1::crh-1β::FLAG*	Lakhina et al., 2015	CQ159
C. elegans strain CQ160: *crh-1(tz2); wqEx29 [Pmyo-2::mCherry]/PuroR; Pceh-24::crh-1β::FLAG*	Lakhina et al., 2015	CQ160
C. elegans strain CQ161: *pCRE::GFP*	Suo et al., 2006	CQ161
C. elegans strain JN897: *Podr-1::egl-30(Q205L)*	Matsuki et al., 2006	JN897
C. elegans strain JN819: *Podr-1::goa-1(Q205L)*	Matsuki et al., 2006	JN819
C. elegans strain IV183: *ueEx104 [odr-3::unc-31sense::sl2mCherry, odr-3::unc-31antisense::sl2mCherry, unc-122::RFP]*	Leinwand and Chalasani., 2013	IV183
C. elegans strain IV8: *ueEx4 [odr-3::eat-4 sense, odr-3::eat-4 antisense, eat-2::GFP]*	Leinwand and Chalasani., 2013	IV8
C. elegans strain CX9735: *gcy-28(tm2411);kyEX2139[odr-3::pkc1(A160E)::sl2GFP, elt-2::GFP]*	Tsunozaki et al., 2008	CX9735
C. elegans strain CQ210: *egl-30(js126); crh-1(tz2)*	This paper	CQ210
C. elegans strain CQ243: *egl-30(js126); crh-1(tz2);wqEx29 [Pmyo-2::mCherry]/PuroR;Pceh-24::crh-1β::FLAG*	This paper	CQ243
C. elegans strain CQ245: *egl-30(js126); crh-1(tz2);wqEx29 [Pmyo-2::mCherry]/PuroR;Pmbr-1::crh-1β::FLAG*	This paper	CQ245
C. elegans strain CQ252: *egl-30(js126);wqEx28[pCRE::GFP]*	This paper	CQ252
C. elegans strain CQ253: *egl-30(js126);Podr-1::goa-1(Q205L)*	This paper	CQ253
C. elegans strain CQ294: *egl-8(n488);Podr-1::egl-30(Q205L)*	This paper	CQ294
C. elegans strain CQ406: *mbr-1(qa5901);Podr-1::egl-30(Q205L)*	This paper	CQ406
C. elegans strain CQ407: *egl-30(js126);ueEx104[odr-3::unc-31sense::sl2mCherry,odr-3::unc-31antisense::sl2mCherry,unc-122::RFP]*	This paper	CQ407
C. elegans strain CQ412: *egl-30(js126);ueEx4[odr-3::eat-4 sense, odr-3::eat-4 antisense,eat-2::GFP*	This paper	CQ412
C. elegans strain CQ415: *crh-1(tz2);Podr-1::egl-30(Q205L)*	This paper	CQ415
C. elegans strain CQ465: *ttx-3(ot22);Podr-1::egl-30(Q205L)*	This paper	CQ465
C. elegans strain CQ547: *Podr-1::egl-30(V180M);pCRE::GFP*	This paper	CQ547
C. elegans strain CQ563: *Podr-3::pkc1(A160E)::sl2GFP, elt-2::GFP*	This paper	CQ563
C. elegans strain CQ477: *Podr-1::egl-30(V180M)*	This paper	CQ477
C. elegans strain CQ429: *pHSP16-48::FLPase; Podr-1::FRT::egl-30(Q205L); Pmyo-2::mCherry*	This paper	CQ429
C. elegans strain CQ430: *pHSP16-48::FLPase; Podr-1::FRT::egl-30(Q205L);Pmyo-2::mCherry #2*	This paper	CQ430
Oligonucleotides		
pmp-3 qPCR Forward primer AGTTCCGGTTGGATTGGTCC	This paper	N/A
pmp-3 qPCR Reverse primer CCAGCACGATAGAAGGCGAT	This paper	N/A
hsp-70 qPCR Forward primer CCGGTTGAAAAGGCACTTCG	This paper	N/A
hsp-70 qPCR Reverse primer GAGCAGTTGAGGTCCTTCCC	This paper	N/A
crh-1 qPCR Forward primer CCACAACAAAACGGACTCGG	This paper	N/A
crh-1 qPCR Reverse primer ATGAGCCCAGATGTGCCTTC	This paper	N/A
Recombinant DNA		

REAGENT or RESOURCE	SOURCE	IDENTIFIER
Plasmid: pL4440 RNAi control	Ahringer RNAi library	N/A
Plasmid: pL4440-*ttx-3* RNAi	Ahringer RNAi library	N/A
Software and Algorithms		
PUMAdb	Princeton University MicroArray database	http://puma.princeton.edu
Cluster 3.0	Eisen et al., 1998	http://bonsai.hgc.jp/~mdehoon/software/cluster/software.htm
NIS-Elements AR	Nikon Instruments	https://www.nikoninstruments.com/Products/Software/NIS-Elements-Advanced-Research
Prism 7	Graphpad Prism	https://www.graphpad.com/scientific-software/prism/
Other		
C. elegans (V2) Gene Expression Microarray, 4x44K	Agilent	Cat# G2519F-020186